MEMBRANE TRANSPORT STRUCTURE FUNCTION AND BIOGENESIS:

Direct Interaction of Dermaseptin S4 Aminoheptanoyl Derivative with Intraerythrocytic Malaria Parasite Leading to Increased Specific Antiparasitic Activity in Culture

Leah Efron, Arie Dagan, Leonid Gaidukov, Hagai Ginsburg and Amram Mor

J. Biol. Chem. 2002, 277:24067-24072.
doi: 10.1074/jbc.M202089200 originally published online April 5, 2002

THE JOURNAL OF BIOLOGICAL CHEMISTRY

Vol. 277, No. 27, Issue of July 5, pp. 24067–24072, 2002
Printed in U.S.A.

Direct Interaction of Dermaseptin S4 Aminoheptanoyl Derivative with Intraerythrocytic Malaria Parasite Leading to Increased Specific Antiparasitic Activity in Culture*

Received for publication, March 4, 2002, and in revised form, March 25, 2002
Published, JBC Papers in Press, April 5, 2002, DOI 10.1074/jbc.M202089200

Leah Efron, Arie Dagan, Leonid Gaidukov, Hagai Ginsburg‡, and Amram Mor

From the Institute of Life Sciences, The Hebrew University of Jerusalem, Givat Ram 91904 Jerusalem, Israel

Antiplasmodial activity of the dermaseptin S4 derivative K_4S4(1–13) (P) was shown to be mediated by lysis of the host cells. To identify antiplasmodial peptides with enhanced selectivity, we produced and screened new derivatives based on P and singled out the aminoheptanoylated peptide (NC7-P) for its improved antiplasmodial properties. Compared with P, NC7-P displayed both increased antiparasitic efficiency and reduced hemolysis, including against infected cells. Antiplasmodial activity of P and its derivative was time-dependent and irreversible, implying a cytotoxic effect. But, whereas the dose dependence of growth inhibition and hemolysis of infected cells overlapped when treated with P, NC7-P exerted more than 50% growth inhibition at peptide concentrations that did not cause hemolysis. Noticeably, NC7-P but not P, dissipated the parasite plasma membrane potential and caused depletion of intraparasite potassium at nonhemolytic conditions. Confocal microscopy analysis of infected cells localized the rhodaminated derivative in association with parasite membranes and intraerythrocytic tubulovesicular structures, whereas in normal cells, the peptide localized exclusively at the plasma membrane. Overall, the data demonstrate that antimicrobial peptides can be engineered to act specifically on the membrane of intracellular parasites and support a mechanism whereby NC7-P crosses the host cell plasma membrane and disrupts the parasite membrane(s).

Malaria constitutes the most widespread infectious disease affecting hundreds of million people, causing the death of one million children every year in Africa alone (1). Because this dreadful situation could worsen because of the increasing resistance of parasites to available antiplasmodial drugs, new drugs must be developed.

Antimicrobial peptides have recently emerged as interesting tools for exploring new antimalarial targets (2–6). These ubiquitous peptides vary considerably in structure, size, amino acid sequence, and spectrum of action (7–11), but the most potent peptides always have a pronounced amphipathic and distinctly basic character (12–16). They are believed to exert cytolytic action through their effect on the membrane of target cells by a mechanism whose details remain to be fully understood. Antimicrobial action is not mediated by interaction with stereospecific targets such as receptors or enzymes (3, 17). Apparently, their charge and hydrophobicity are the main features affecting cytotoxicity (18–20). Some antimicrobial peptides were stipulated to form ion channels or pores (21, 22). Various basic models for a membranolytic mechanism were proposed ranging from pore formation to induction of structural defects (20–27) that lead to membrane permeabilization. Consequently, essential ions and metabolites are free to leak in and out and to dissipate the electric potential across the membrane, eventually leading to cell death.

Antimicrobial peptides often display a broad spectrum of activity affecting Gram-negative and Gram-positive bacteria, yeast and filamentous fungi, some enveloped viruses, and many types of cancer cells. Yet many are relatively inactive on normal eukaryotic cells (28–30). Although the basis for this discrimination is also unclear, it appears to be related to the lipid composition of the target membrane (*i.e.* fluidity, negative charge density, and the absence or presence of cholesterol) and the presence in the peptide-susceptible organisms of a large negative *trans*-membrane electrical potential (31–34). Such a peptide-based antimicrobial system has attractive advantages over classical antibiotics because it makes it extremely difficult for microbial targets to develop resistance (15, 35, 36). Nevertheless, a major drawback of such an antimicrobial system is reflected in its unselective activity over a wide range of cell types, which could be problematic, for instance, in systemic routes of administration (37).

Dermaseptin S4 is a 28-residue antimicrobial peptide isolated from frog skin (38). The native peptide was shown to exert antiplasmodial activity (4), whereas subsequent studies (17, 39) identified a 13-residue derivative, K_4-S4(1–13), displaying a considerable *in vitro* effectiveness on *Plasmodium falciparum*, the most lethal human parasite (5). The antiplasmodial action was rapid and was shown to be mediated by permeabilization of host cell plasma membrane. Although K_4-S4(1–13) was less hemolytic to normal erythrocytes, it was deemed necessary to develop additional derivatives that could affect the parasite with minimal threat to erythrocytes. Recently, acyl derivatives of K_4-S4(1–13) were shown to increase antiplasmodial activity, although the most potent antiparasitic peptides still displayed high hemolytic activity (6). In this study, a series of new dermaseptin S4 derivatives based on K_4-S4(1–13) were produced and investigated for antiplasmodial and hemolytic properties. After screening for the most selective compound, we investigated its detailed mechanism of action.

MATERIALS AND METHODS

Synthesis of Dermaseptin S4 Derivatives—The reference peptide K_4-S4(1–13) was synthesized by the solid phase method, applying the

* This work was supported by Israel Science Foundation Grant 523/98. The costs of publication of this article were defrayed in part by the payment of page charges. This article must therefore be hereby marked "*advertisement*" in accordance with 18 U.S.C. Section 1734 solely to indicate this fact.

‡ To whom correspondence should be addressed: Dept. of Biological Chemistry, Inst. of Life Sciences, The Hebrew University of Jerusalem, Givat Ram 91904 Jerusalem, Israel. E-mail: hagai@vms.huji.ac.il.

Fmoc[1] active ester chemistry on a fully automated, programmable peptide synthesizer (model 433A; Applied Biosystems) as described (17) with the following modifications. 4-Methylbenzhydrylamine resin (Novabiochem) was used to obtain amidated peptides. The various analogs were prepared by linking the N terminus of K_4-S4(1–13) to one of the compounds detailed in Table I as follows. After removing the Fmoc group (20% piperidine/*N*-methylpyrrolidone), the resin-bound peptide (20 mg) was suspended in 0.7 ml of dimethylformamide to which a 2-fold molar excess of the relevant *tert*-butyloxyl-carbonyl protected amino-carboxylic acid was added followed by 3-fold molar excess of 1-ethyl-3-(dimethylaminopropyl)carbodiimide. In the specific case of t-BOC aminolauric acid, reactants were mixed in dimethylformamide/CH_2Cl_2 (1:1). The reaction mixture was sonicated for 5 min and then agitated for 24 h at room temperature. The resin was washed with dimethylformamide and then with ether/dichloromethane (1:1) and dried for 4 h at 50 °C. For visualization studies, rhodamine was covalently attached to the deprotected N terminus of NC6-P (Table I) while still linked to the resin. Peptide labeling, cleavage from the resin, and purification by HPLC were also performed as described (17). The purified peptides were subjected to amino acid analysis and mass spectrometry to confirm their composition. Peptides were stocked as lyophilized powder at −20 °C. Prior to testing, fresh solutions were prepared in water, briefly vortexed, sonicated, centrifuged, and then diluted in the appropriate medium.

Determination of Hemolytic Potential—Human blood was rinsed three times in PBS (50 mM sodium phosphate, 150 mM NaCl, pH 7.3) by centrifugation for 1 min at 2700 × *g*, and then 2.5×10^8 red blood cells (RBC) suspended in 50 μl PBS were added to Eppendorf test tubes containing 200 μl of peptide solutions (serial 2-fold dilutions in PBS), PBS alone (for baseline values), or distilled water (for 100% hemolysis). After incubation (3 h under agitation, 37 °C) the samples were centrifuged, and the hemolytic activity was assessed as a function of hemoglobin leakage by measuring the absorbance of 200 μl of supernatant (405 nm). The statistical data were obtained from at least three independent experiments performed in duplicate.

Parasite Cultivation—The W2 strain of *P. falciparum* was cultivated as described (40) using human RBC. The culture was synchronized by the sorbitol method (41) using the less toxic alanine, and infected cells were enriched from culture by Percoll-alanine gradient centrifugation (40).

Drug Screening Test—Synchronized cultures at the ring stage were cultured at 1% hematocrit and 2% parasitemia in the presence of 10 μM of dermaseptin derivatives. After 18 h of incubation, parasite viability was determined by [^{3}H]hypoxanthine (Hx) uptake (final concentration, 2 μCi/ml) during 6 h and compared with controls (without peptide). Parallel cultures were tested after 6 h for hemolysis as determined by hemoglobin absorbance at 405 nm and compared with cells lysed in water.

Determination of IC_{50}—Parasite viability in the presence of increasing peptide concentrations was determined as described above. The 50% inhibitory concentration (IC_{50}) was determined by nonlinear regression fitting of the data using Sigmaplot. The same procedures were used for the measurement of parasite viability and hemolysis and the stage and the time dependence of drug effect at the different stages.

Peptide-mediated Dissipation of Parasite Membrane Potential—Trophozoite stage culture in modified growth medium (wash medium containing 10 mM bicarbonate and 7% plasma) at 0.5% hematocrit was incubated in the presence of 1 μM rhodamine 123 for 30 min at 37 °C. Rhodamine 123 accumulates inside cells in proportion to the membrane potential ($\Delta\Psi$) and has been shown to respond to the dissipation of the plasma membrane $\Delta\Psi$ in *P. falciparum* (42). Aliquots of this culture were then exposed to P, NC7-P, or a mixture of 10 μM nigericin (K^+:H^+ exchanger) and 10 μM monensin (Na^+:H^+ exchanger) to dissipate the ion gradient across membranes (positive control). The samples were taken at different time intervals, and the cells were washed in PBS and resuspended in original sample volume of PBS. Aliquots of 120 μl were placed in a 96-well plate and read in a fluorescence reader (excitation wavelength λ_{ex} = 530 nm, emission wavelength λ_{em} = 585 nm). Relative fluorescence (as a percentage of that of the untreated control at the same time) was plotted against the time of incubation.

Peptide-mediated Depletion of Parasite Intracellular Potassium—Infected cells at the young trophozoite stage were enriched from culture using the Percoll-alanine gradient (97% parasitemia, determined on Giemsa-strained thin blood smears) and incubated at 0.5% hematocrit in culture medium at 37 °C, with or without 10 μM P or NC7-P. At time 0 and after 4 h, aliquots were taken, cells were washed in PBS, and parasites were freed by saponine (0.003% w/v in PBS)-induced lysis for several minutes at room temperature. The parasites were washed several times in PBS and finally washed with 110 mM $MgCl_2$ buffered with 10 mM Hepes. The parasites were disrupted by freezing and thawing, and potassium content in the supernatant was determined by inductive-coupled plasma atomic emission spectroscopy on an Optima 3300 Inductively coupled plasma atomic emission spectroscopy system (PerkinElmer Life Sciences).

Intracellular Localization of Fluorescent Peptide by Confocal Microscopy—Cultures (1% hematocrit) of trophozoites (~ 90% parasitemia) and uninfected human erythrocytes were incubated in the presence of the rhodaminated peptide at 1 and 10 μM. After 15 and 120 min, the cells were washed and analyzed. In control experiments, the cells were incubated in the presence of free rhodamine and unlabeled NC7-P under similar conditions. Confocal microscope images of the samples (nonfixed cells) were taken using an MRC 1024 confocal imaging system (Bio-Rad). The microscope (Axiovert 135M; Zeiss) is equipped with a 63× objective (Apoplan; NA 1,4). For rhodamine excitation, an Argon ion laser adjusted at 514 nm (emission wavelength = 580 ± 32 nm) was used.

TABLE I
Structure of the parent peptide P and its derivatives

Peptide	Structure	Designation
K_4-S4(1-13)$_{NH2}$	[1]ALWKTLLKKVLKA$_{amide}$	P
Glycyl-P	H_2N-CH_2-CO-**P**	NC2-P
Aminobutyryl-P	H_2N-$(CH_2)_3$-CO-**P**	NC4-P
Aminoheptanoyl-P	H_2N-$(CH_2)_6$-CO-**P**	NC7-P
Aminolauroyl-P	H_2N-$(CH_2)_{11}$-CO-**P**	NC12-P
Lysyl-P	H_2N-CH-CO-**P** \ $(CH_2)_4$-NH_2	N2C6-P
Diaminopropanoyl-lysyl-P	H_2N \ HC-CH_2-CONH-CH-CO-**P** H_2N / \ $(CH_2)_4$-NH_2	N4C9-P

[1] Amino acid sequence in the one letter code.

RESULTS

To reduce hemolytic activity, acylated peptides (6) were converted to aminoacyl derivatives. Identity of the synthetic products (Table I) was confirmed by mass analysis of the HPLC-purified peptides (purity was > 95%). As shown in Fig. 1*A*, acylation of P resulted in increased hydrophobicity concomitant with increased acyl chain length. Comparatively, aminoacyl analogs had reduced hydrophobicity, presumably because of their increased polarity. Fig. 1*B* shows that increased hydrophobicity of acyl derivatives first counteracts the hemolytic activity of the parent peptide (as measured in PBS) and thereafter increases it. The aminoacyl derivatives display similar biphasic effect albeit at considerably higher concentrations. It is suggested that the biphasic effect results from the opposing forces of membrane solubilization (enhanced by acyl chain length) and surface aggregation (essential for hemolytic activity) (11).

Screen of Antiplasmodial and Hemolytic Activities—To identify peptides that will selectively kill the parasite without lysis of the host cell, the aminoacyl peptides were screened at a single dose of 10 μM for antiplasmodial and hemolytic activities. All of the peptides tested inhibited plasmodial growth to various extents. But, whereas derivatives with short hydrocarbon chains had either lower (*e.g.* NC2-P) or similar (*e.g.* NC4-P)

[1] The abbreviations used are: Fmoc, *N*-(9-fluorenyl)methoxycarbonyl; RBC, red blood cells; PBS, phosphate-buffered saline; Hx, hypoxanthine; P, K_4-S4(1–13); HPLC, high performance liquid chromatography.

antiplasmodial activity compared with the parent peptide P, the more hydrophobic peptides NC7-P and NC12-P were more active (Fig. 2*a*). Yet although derivatives with 2–7 hydrocarbons (NC2-P, NC4-P, and NC7-P) were less hemolytic, NC12-P displayed increased hemolytic action (Fig. 2*b*). To select for the most suitable derivative, we compared the ratio of relative inhibition to relative hemolysis. This analysis (Fig. 2*c*) revealed that NC4-P and NC7-P were the most selective, *i.e.* the antiplasmodial activity was superior to the hemolytic action.

Two additional branched derivatives (N2C6-P and N4C9-P) were prepared to assess the effect of modulating the charge and hydrophobicity. Compared with P, N2C6-P did not display improved antiplasmodial activity but resulted in increased hemolysis, whereas N4C9-P displayed reduced antiplasmodial and hemolytic activities (Fig. 2, *a* and *b*). Because NC7-P combined both increased antiplasmodial effect with lower hemolysis compared with P (as reflected by the increased ratio of the percentage of inhibition to the percentage of lysis in Fig. 2*c*), this derivative was chosen for further and more detailed investigations.

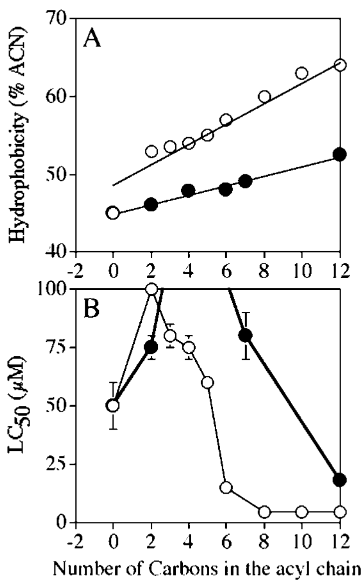

FIG. 1. **Hydrophobicity and hemolytic potential of two groups of acyl-peptides.** *A* shows the effect of chain length on hydrophobicity, measured as function of the acetonitrile (*ACN*) concentration required for elution of acyl (○) and aminoacyl (●) derivatives, using a linear gradient of acetonitrile (1%/min) in reversed-phase HPLC with a C4 column. *B* shows the peptide concentrations that produced 50% hemolysis after 3 h of incubation in PBS. The *error bars* represent the *standard deviations* from the mean calculated from at least two independent experiments performed in duplicate. If no error bar is shown, the standard deviation was smaller than the diameter of the symbol.

Detailed Determination of Antiplasmodial Activity and Stage Dependence of Selected Compounds—The dose response of NC7-P was investigated and compared with the parent peptide P using synchronized cultures of *P. falciparum* that were exposed to the peptides either at the ring or at the trophozoite stage. NC7-P was more effective than P at the ring stage (IC_{50} = 5.3 ± 0.7 and 7.7 ± 0.9 μM, respectively), but the opposite was observed for the trophozoite stage (IC_{50} = 6.2 ± 0.5 and 3.4 ± 0.3 μM, respectively). The stage dependence results indicated that ring stage parasites were less sensitive to P, as previously observed (5), than the more mature trophozoite stage. This was not observed with NC7-P. Moreover, the slopes of the dose-response curves were slightly higher for NC7-P (1.9 ± 0.5 and 2.3 ± 0.4, respectively) compared with P (1.5 ± 0.2 and 1.4 ± 0.1, respectively), indicating some differences in the stoichiometry of drug and target relations.

Time Dependence and Reversibility of Antiplasmodial Action—NC7-P (10 μM) was found to be similarly active, and its action was time-dependent both for ring and trophozoite stages, displaying maximal activity after 24 h of exposure (Fig. 3). Removal of the peptide from the culture after 5 h of incubation and measuring parasite viability 19 h later, revealed that the antiplasmodial effect proceeded further even in the absence of peptide in the medium. These results suggest that internalized peptide (see below) could not be removed from the cells and that the antiplasmodial effect was cytotoxic.

Hemolytic Activity versus Antiplasmodial Activity—To further understand the mechanism of antiplasmodial activity, P and NC7-P were tested simultaneously for their hemolytic and antiplasmodial activities. Infected cells at the young trophozoite stage were enriched (~90% parasitemia) from culture and exposed (0.5% hematocrit) to increasing peptide concentrations. Parasite viability was determined after 2 h of exposure to peptides followed by 4 h of exposure to hypoxanthine in culture conditions, whereas hemolysis was assayed on normal and infected erythrocytes after 6 h of exposure to the peptide. Under these conditions of short time exposure of trophozoite-enriched cultures, NC7-P was more inhibitory than P (IC_{50} = 14.2 ± 0.5 and 19.6 ± 1.6 μM, respectively). Yet NC7-P was much less hemolytic than P to infected erythrocytes (LC_{50} = >60 and 21.2 ± 0.6 μM, respectively), whereas this discrepancy was less pronounced for uninfected cells (Fig. 4).

Peptide-mediated Dissipation of the Parasite Plasma Membrane Potential and Induced Leak of Intraparasite Potassium—The fluorescent dye rhodamine 123 accumulates in parasites in correlation with the parasite membrane ΔΨ, and permeabili-

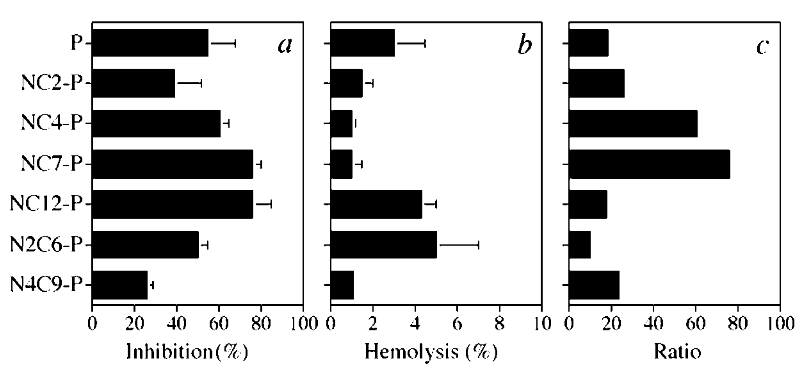

FIG. 2. **Screen of antiplasmodial and hemolytic activities.** Synchronized cultures at the ring stage (2% parasitemia) were cultured in the presence of the designated peptides. After 24 h of incubation, the cultures were divided into two sets. To one set Hx was added, and cell-associated radioactivity was determined and compared with controls (*a*). The second set was used to determine the concentration of hemoglobin in the supernatant compared with fully hemolyzed cultures (*b*). The *error bars* represent the standard deviations from the mean, calculated from at least two independent experiments performed in quadruplicate. *c* shows the ratio of *a*/*b* calculated from the mean values of *a* and *b*.

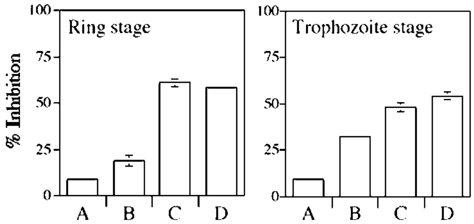

FIG. 3. **Stage dependence of the antiplasmodial activity.** Infected cells were exposed to NC7-P, and parasite growth was determined by Hx incorporation using one of the following procedures. *Columns A*, exposure to NC7-P (5 h) was followed by wash and Hx incorporation (5 h). *Columns B*, exposure to NC7-P (5 h) was followed by wash, recovery without peptide (19 h), and Hx incorporation (5 h). *Columns C*, exposure to NC7-P (24 h) was followed by wash and Hx incorporation (5 h). *Columns D*, exposure to NC7-P (29 h) was directly followed by Hx incorporation (5 h). Each experiment was performed twice in duplicate. The *error bars* represent the standard deviations from the mean.

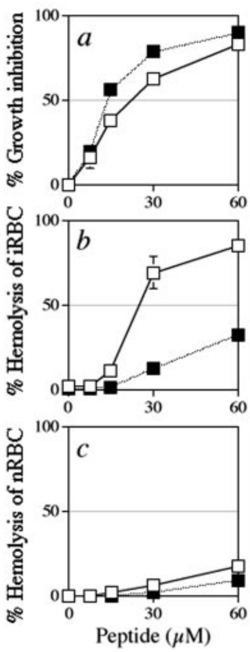

FIG. 4. **Hemolytic activity *versus* antiplasmodial activity.** Infected (*iRBC*) and uninfected cells (*nRBC*) were cultured with peptides for 2 h and then with Hx for 4 h, and the cell-associated radioactivity was determined on one set (*a*). Hemolysis was determined after 6 h of incubation in two additional sets of cultured infected RBC (*b*) and uninfected RBC (*c*). □, *P*; ■, NC7-P. Each experiment was performed at least twice in quadruplicate. The *error bars* represent the standard deviations from the mean. If no error bar is shown, the standard deviation was smaller than the diameter of the symbol.

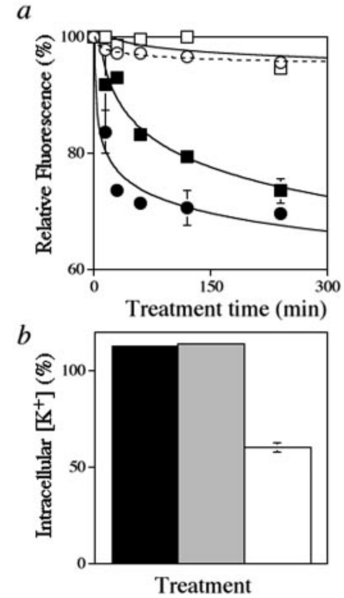

FIG. 5. **Peptide-mediated dissipation of parasite membrane potential and depletion of parasite intracellular potassium.** *a*, trophozoites (97% parasitemia) preincubated with rhodamine 123 were exposed to PBS (○), P (□), or NC7-P (■) or to a mixture of known ionophores: nigericin + monensin (●). The samples were taken at different time intervals, washed, and resuspended in the original sample volume of PBS. Their relative fluorescence (as the percentage of untreated control at the same time) is plotted against the time of exposure. *b*, infected cells were cultured in absence (*black bar*) or presence of P (*gray bar*) or NC7-P (*white bar*), and parasites were freed from their host cell by saponin lysis. Free parasites were disrupted by freezing and thawing, and the potassium content in the supernatant was determined by inductively coupled plasma atomic emission spectroscopy. The results are shown as percentages of potassium content relative to control at time 0. Each experiment was performed twice in duplicate. The *error bars* represent the standard deviations from the mean.

zation of the parasite membrane by the peptide is expected to reduce $\Delta\Psi$ and thus dye accumulation, as attested by the effect of the ionophores nigericin and monensin (Fig. 5*a*). No dissipation of $\Delta\Psi$ was observed with P, whereas NC7-P caused a discernible reduction. Moreover, exposure of infected cells (~90% parasitemia) to 10 μM peptides and measurement of potassium content in saponin-freed parasites revealed no effect of P and a marked reduction in the presence of NC7-P (Fig. 5*b*). The congruity of both types of results clearly indicates that at nonhemolytic concentrations NC7-P but not P can cross the host cell membrane without upsetting it and interact with the parasite plasma membrane to permeabilize it.

Subcellular Localization of the Peptide Using a Rhodaminated Derivative—A fluorescent peptide where rhodamine was covalently linked to the N terminus of the peptide was prepared and compared with NC7-P with respect to antiplasmodial and hemolytic activities as described above. The rhodaminated peptide had similar antiplasmodial activity, but it was considerably more hemolytic than NC7-P (data not shown). Inspection by confocal microscopy (mid-depth Z slice) of uninfected human erythrocytes exposed to 1 or 10 μM labeled peptide for up to 2 h under culture conditions revealed intense labeling of many cells (Fig. 6*a*). The dye was seen associated exclusively with the erythrocyte membrane. Fluorescence intensity increased with concentration, but the number of labeled cells remained practically unchanged with time (not shown). Similar exposure of trophozoite-infected human erythrocytes (~90% parasitemia) labeled many more cells with the same pattern of dose and time dependence seen with uninfected erythrocytes (Fig. 6*b*). Further magnifications disclosed that the label was specifically localized in the parasites and that labeling existed in the host compartment of inclusions that can be identified as tubulovesicular structures and Maurer's clefts. In control experiments where the cells were incubated under similar conditions but in the presence of 10 μM free rhodamine and 10 μM unlabeled NC7-P, neither the infected nor the normal cells were labeled.

DISCUSSION

To design dermaseptin derivatives with greater selectivity, we have been guided by the following rationale. Selective activity of antimicrobial peptides demonstrably depends on the membrane lipid composition (17–27). The lipid composition of the infected cell is considerably different from that of uninfected erythrocytes and other somatic cells of the host in that it is devoid of cholesterol and it has considerably less sphingomylin and phosphatidyl serine, larger concentrations of phos-

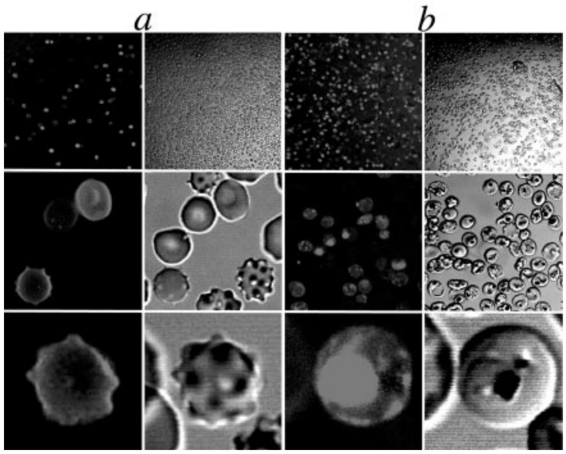

FIG. 6. **Localization of the fluorescent peptide by confocal microscopy.** Normal human erythrocytes and trophozoites (~90% parasitemia) were exposed to the rhodaminated peptide and then washed and analyzed unfixed by confocal microscopy. Three zoom levels of the same microscopic field are shown (increasing from *top* to *bottom*). Each zoom level shows both the fluorescence (*left column*) and the light transmission (*right column*) of the same image for normal (*a*) and infected cells (*b*).

phatidylcholine, phosphatidylethanolamine, and phosphatidylinositol, and a decreased level of unsaturation of the fatty acids (43). Although the lipid compositions of host and parasite membrane are similar, the potential of the parasite membrane is considerably higher than that of the host cell membrane (42), and it is in the right polarity needed for enhancement of peptide incorporation (32–34). Thus, we hypothesized that the discriminating effect of the dermaseptin derivative could be exerted on two additional levels: (i) preference for infected cells because of lipid composition and (ii) the preference for the parasite membrane because of favorable $\Delta\Psi$ once inside the cytosol of the infected cell. Increasing the lipophilicity of the peptide will render it more permeable through the host cell membrane and therefore more accessible to the parasite membrane. Because this feature also increases hemolytic activity (6, 17), we have used aminoacyl moieties to reduce hydrophobicity and, hence, the risk for hemolysis.

This reasoning has been tested experimentally using seven peptides of varying N termini. For all derivatives the antiplasmodial and hemolytic activities were found to depend on the nature of the added moiety. Sorting the derivatives by their selectivity (ratio of the percentage of inhibition to the percentage of hemolysis), NC7-P was singled out as the most selective and was further used in parallel with the parent peptide P for detailed investigations. To acquire a deeper understanding of the selectivity effect, parallel determination of antiplasmodial activity and lysis of normal and infected erythrocytes were conducted for short incubation times. The IC_{50} values obtained in these experiments were understandably higher than those obtained in the standard dose-response test that lasted 24 h because of the time dependence effect and the increased number of infected cells (from 2 to ~90%, respectively). Outstandingly, whereas with P the dose dependence of growth inhibition and lysis of infected cells overlapped, with NC7-P more than 50% growth inhibition occurred at concentrations that did not cause lysis at all. This discrepancy is possibly even larger because both growth inhibition and lysis are time-dependent processes, and exposure to peptides was only 2 h in the first case and 6 h in the second. Noticeably, whereas P was more lytic to infected cells than to uninfected cells, such discrepancy was much less pronounced for NC7-P. This is a further demonstration of the lipid-dependent specificity of peptides.

Unlike P (5), NC7-P was not stage-selective, being equally inhibitory for both the young ring stage and the more mature trophozoites. We propose that P acts essentially by lysing the host cell membrane. It is more lytic to host cells harboring mature parasite stages, indicating dependence on changes induced by parasite in the host cell membrane. Because the latter evolves with parasite maturation, throphozoites are expected to be more sensitive than rings, as was found (5). In contrast, the selectivity of the NC7-P seems to depend on the differential $\Delta\Psi$ of host and parasite membrane. Because this is established from the onset of parasite development, the permeable peptide is always sucked into the parasite membrane and affects it. For this reason stage dependence with NC7-P is neither expected nor observed.

The antiplasmodial effect of NC7-P was clearly time-dependent. It was found to have a stage-independent cytotoxic activity that persisted and accrued even when it was discarded from the culture. This indicates that the association of NC7-P with the parasite membrane is essentially irreversible and that even without saturation of the putative peptide binding sites, it results in the continuous loss of the parasites viability because of membrane permeabilization. The interaction of a fluorescent analog of NC7-P with uninfected erythrocytes was seen to be localized at the cell membrane. However, we cannot exclude the possibility that if the peptide was internalized, its fluorescence was quenched by hemoglobin. In infected cells, the fluorescent analog reached the parasite and labeled its plasma membrane and the tubulovesicular network that emerges from the parasitophorous vacuolar membrane and extends to the erythrocyte membrane (44, 45). The high resolution images obtained by fluorescence confocal microscopy recall the subcellular distribution of the fluorescent phospholipid NBD-PC (46), attesting to the association of the peptide with the membranes of the infected cell. Parenthetically, the staining of a subpopulation of infected cells conforms with partial inhibition of parasite growth as measured by the hypoxanthine viability assay that integrates the response of the entire parasite population. To the best of our knowledge, this is the first demonstration ever of an antiplasmodial compound that acts on a subpopulation of cells in an all-or-none fashion rather than reducing vital processes in each cell.

The lipophilic and membrane-trophic character of NC7-P insinuates that its interaction with the parasite membrane would lead to nonselective permeabilization. The observed dissipation of $\Delta\Psi$ could result from increased permeability to protons because the major generator of $\Delta\Psi$ is presumably the V-type H^+ pump (47, 48). Permeabilization to protons undercuts the function of the pump as the major regulator of cellular pH. Short circuiting of the electrogenic function of the pump presumably underlies the observed loss of cellular potassium, the maintenance of which seems to depend on $\Delta\Psi$. Although these presumptions could explain the gradual and irreversible loss of vital cellular functions, we cannot exclude at the present time the possibility that NC7-P acts on a different cellular target that mediates its cytotoxic action.

In conclusion, we demonstrate in this investigation that membrane active peptides can be engineered to act specifically on the membrane of the intracellular parasite to perturb its functions. This selective activity reduces the potential harm from inadvertent lysis of the erythrocytes of the host. This is a major achievement in the fine tuning of peptide composition toward its further development as a potential antimalarial drug. It has been shown previously that intravenous administration of P to rats was well tolerated at least up to 10 mg/kg (39) and that the LD_{50} of S4 derivatives (including P) administered intraperitoneally in mice was 25 mg/kg, whereas effectiveness against *Pseudomonas aeruginosa*-induced peritonitis was achieved at ≤4.5 mg/kg (49). Because NC7-P is less hemolytic than P, it can be assumed that it will be less toxic *in vivo*. Such concentrations are substantially higher than the IC_{50} of NC7-P against the malaria parasite, indicating that it could also be effective *in vivo*. It remains to be shown experimentally that NC7-P is not toxic to mammalian cells or to whole animals and that its antiplasmodial effect is maintained *in vivo*. Investigations of these aspects are underway in our laboratory.

Acknowledgments—The expert assistance of Dr. Naomi Melamed and Josephina Silfen (Hebrew University) in confocal microscopy and peptide synthesis, respectively, is gratefully acknowledged.

REFERENCES

1. World Health Organization (1999) *Disease Statistics World Health Report*, *www.who.int/whr/1999/en/disease.htm*
2. Jaynes, J. M., Burton, C. A., Barr, S. B., Jeffers, G. W., Julian, G. R., White, K. L., Enright, F. M., Klei, T. R., and Laine, R. A. (1988) *FASEB J.* **2,** 2878–2883
3. Wade, D., Boman, A., Wahlin, B., Drain, C. M., Andreu, D., Boman, H. G., and Merrifield, R. B. (1990) *Proc. Natl. Acad. Sci. U. S. A.* **87,** 4761–4765
4. Ghosh, J. K., *et al.* (1997) *J. Biol. Chem.* **272,** 31609–31616
5. Krugliak, M., Feder, R., Zolotarev, V., Gaidukov, L., Dagan, A., Ginsburg, H., and Mor, A. (2000) *Antimicrob. Agents Chemother.* **44,** 2442–2451
6. Dagan, A., Efron L., Gaidukov L., Mor A., and Ginsburg H. (2002) *Antimicrob. Agents Chemother.* **46,** 1059–1066
7. Ganz, T., and Lehrer, R. (1998) *Curr. Opin. Immunol.* **10,** 41–44
8. Hancock, R. E. W., and Chapple, D. S. (1999) *Antimicrob. Agents Chemother.* **43,** 1317–1323
9. Levy, O. (2000) *Blood* **96,** 2664–2672
10. Mor, A. (2001) *The Kirk-Othmer Encyclopedia of Chemical Technology*, *www.mrw.interscience.wiley.com/kirk/articles/peptwise.a01/frame.html*
11. Zasloff, M. (2002) *Nature* **415,** 389–395
12. Maloy, L. W., and Kari, U. P. (1995) *Biopolymers* **37,** 105–122
13. Nicolas, P., and Mor, A. (1995) *Annu. Rev. Microbiol.* **4,** 277–304
14. Tossi, A., Sandri, L., and Giangaspero, A. (2000) *Biopolymers* **55,** 4–30
15. Chen, J., Falla, T. J., Liu, H. J., Hurst, M. A., Fujii, C. A., Mosca, D. A., Embree, J. R., Loury, D. J., Radel, P. A., Chang, C. C., Gu, L., Fiddes, J. C. (2000) *Biopolymers.* **55,** 88–98
16. Blondelle E. S., and Lohner K. (2000) *Biopolymers* **55,** 74–87
17. Feder, R., Dagan, A., and Mor, A. (2000) *J. Biol. Chem.* **275,** 4230–4238
18. Mor, A., Hani, K., and Nicolas, P. (1994) *J. Biol. Chem.* **269,** 31635–31641
19. Strahilevitz, J., Mor, A., Nicolas, P., and Shai, Y. (1994) *Biochemistry* **33,** 10951–10960
20. Oren, Z., and Shai, Y. (1998) *Biopolymers* **47,** 451–463
21. Sokolov, Y., Mirzabekov, T., Martin, D. W., Lehrer, R. I., and Kagan, B. L. (1999) *Biochim. Biophys. Acta* **1420,** 23–29
22. Yang, L., Weiss, T. M., Lehrer, R. I., and Huang, H. W. (2000) *Biophys. J.* **79,** 2002–2009
23. Milik, M., and Skolnick, J. (1993) *Proteins* **15,** 10–25
24. Shai, Y. (1995) *Trends Biochem. Sci.* **20,** 460–464
25. White, S. H., and Wimley, W. C. (1998) *Biochim. Biophys. Acta.* **1376,** 339–352
26. Huang, H. W. (2000) *Biochemistry* **39,** 8347–8352
27. Uematsu, N., and Matsuzaki, K. (2000) *Biophys. J.* **79,** 2075–2083
28. Mor, A., and Nicolas, P. (1994) *J. Biol. Chem.* **269,** 1934–1939
29. Martin, E., Ganz, T., and Lehrer, R. I. (1995) *J. Leukocyte Biol.* **58,** 128–136
30. Soballe, P. W., Maloy, W. L., Myrga, M. L., Jacob, L. S., and Herlyn, M. (1995) *Int. J. Cancer.* **60,** 280–284
31. Andreu, D., and Rivas, L. (1998) *Biopolymers* **47,** 415–433
32. Cruciani R. A., Barker J. L., Zasloff M., Chen H. C., and Colamonici O. (1991) *Proc. Natl. Acad. Sci. U. S. A.* **88,** 3792–3796
33. Matsuzaki K., Sugishita K., Fujii N., and Miyajima K. (1995) *Biochemistry* **34,** 3423–3429
34. Diaz-Achirica P., Ubach J., Guinea A., Andreu D., and Rivas L. (1998) *Biochem. J.* **330,** 453–460
35. Lamb, H. M., and Wiseman, L. R. (1998) *Drugs* **56,** 1047–1054
36. Mor, A. (2001) *Drug Dev. Res.* **50,** 440–447
37. Gura, T. (2001) *Science.* **291,** 2068–2071
38. Mor, A., and Nicolas, P. (1994) *Eur. J. Biochem.* **219,** 145–154
39. Feder, R., Nechushtai, R., and Mor, A. (2001) *Peptides* **22,** 1683–1690
40. Kutner, S., Breuer, W. V., Ginsburg, H., Aley, S. B., and Cabantchik, Z. I. (1985) *J. Cell. Physiol.* **125,** 521–527
41. Lambros, C. J., and Vanderberg, J. P. (1979) *J. Parasitol.* **65,** 418–420
42. Tanabe, K., Izumo, A., Kato, M., Miki, A., and Doi, S. (1989) *J. Protozool.* **36,** 139–143
43. Vial, H. J., and Ancelin, M. L. (1998) in *Malaria: Parasite Biology, Pathogenesis and Protection* (Sherman, I. W., ed) pp. 159–175, ASM Press, Washington, D.C.
44. Elmendorf, H. G., and Haldar, K. (1994) *J. Cell Biol.* **124,** 449–462
45. Elford, B. C., and Ferguson, D. J. (1993) *Parasitol. Today* **9,** 80–81
46. Grellier, P., Rigomier, D., Clavey, V., Fruchart, J., and Schrevel, J. (1991) *J. Cell Biol.* **112,** 267–277
47. Mikkelsen, R. B., Tanabe, K., and Wallach, D. F. (1982) *J. Cell Biol.* **93,** 685–689
48. Saliba, K. J., and Kirk, K. (1999) *J. Biol. Chem.* **274,** 33213–33219
49. Navon-Venezia S., Feder R., Gaidukov L., Carmeli Y., and Mor A. (2002) *Antimicrob. Agents Chemother.* **46,** 689–694